The Influence of Air Dilution with Nitrogen on Hydrogen Jet Ignition

Odie Nassar, Surya Kaundinya Oruganti, Marcel Martins Alves
Tel Aviv University, School of Mechanical Engineering
Tel Aviv, 69978, Israel

Sergey Kudriakov, Etienne Studer
DES/ISAS, CEA, Université Paris-Saclay
Gif-sur-Yvette, France

Liel Ishay
Nuclear Research Center Negev
Negev, Israel

Yoram Kozak
Tel Aviv University, School of Mechanical Engineering
Tel Aviv, 69978, Israel

1 Introduction

Pressurized hydrogen jet release into atmospheric air is associated with many engineering applications, such as high-pressure storage vessels [1] and nuclear power plant safety during a severe cooling system malfunction [2]. Discharge of pressurized hydrogen from a vessel into the ambient leads to formation of a strong shock wave, which is followed by the hydrogen jet. At the jet's head, a thin mixing diffusion layer δ between the hot air and the cold expanded hydrogen is formed, which is represented with a simplified sketch in Fig. 1. It is known that self-ignition typically occurs at the diffusion layer [3]. Nevertheless, the self-ignition process is complex and depends on the interplay between the heat release due to chemical reactions, which leads to a temperature rise, and the jet expansion process, which leads to a temperature drop [4]. Moreover, mass diffusion of the much lighter hydrogen into the hot air as well as conduction heat transfer also govern the self-ignition process.

Many efforts were devoted in recent years to explore the problem of self-ignition experimentally. Experiments involved either completely unconfined or confined conditions, where the pressurized jet is released from a tube [1, 5, 6]. It is now well-established that the self-ignition process is influenced by various parameters and, most importantly, by the downstream geometry. For example, the occurrence of ignition is affected by the tube length, hole release diameter, cross-section shape, and the opening process of the pressure vessel [1, 7, 8]. In addition, this unique phenomenon has been studied theoretically

Correspondence to: odai.nassar@hotmail.de

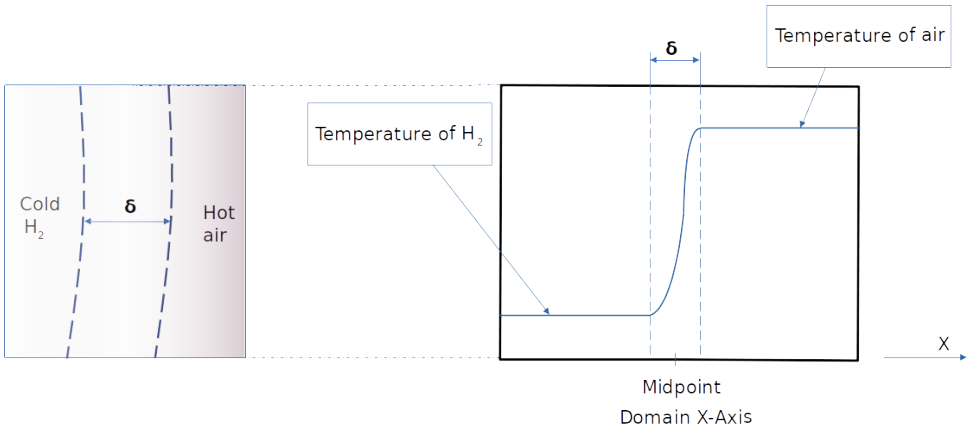

Figure 1: Schematic representation of the diffusion layer at the head of the hydrogen jet.

by various researchers to gain better understanding of the underlying physical phenomena that affect the ignition limits [1, 4].

The scenario of pressurized hydrogen release into air can become even more complicated when the pressurized hydrogen is mixed with other gases and then released into the air. These more involved scenarios include pressurized release of hydrogen-methane [9] or hydrogen-nitrogen mixtures [1]. For both cases, the hydrogen dilution highly affects the ignition delay time. Nevertheless, the effect of inert gas dilution on the air side has never been explored. Thus, in the present work, we address this problem, and explore the effect of nitrogen dilution on the air side. In particular, we carry out and analyze in detail 1-D transient numerical simulations of the ignition process within the diffusion layer at the jet's head.

2 Numerical Solver and Governing Equations

Numerical simulations are conducted via the open source code - Ember. This code is designated for simulating 1-D unsteady reactive flows and provides superior performance for simulations with large multi-step chemical kinetic models [10]. As the diffusion layer is stagnant, in the jet's head frame of reference, see also [4], only the energy and species equations are solved. Thus, the momentum and mass conservation equations are not considered in the current study. The conservation of species is shown in Eq. 1:

$$\rho \frac{\partial Y_k}{\partial t} = -\frac{\partial j_k}{\partial x} + \dot{\omega}_k W_k, \tag{1}$$

where Y_k is the mass fraction of species k, ρ is density, $\dot{\omega}_k$ is the molar production rate of species k, W_k is the molar weight of species k, t is the time, x is the spatial coordinate, and j_k is the diffusive mass flux, which is presented in Eq. 2:

$$j_k = -\rho D_{km} \frac{\partial Y_k}{\partial x} - \frac{D_k^T}{T} \frac{\partial T}{\partial x} + Y_k j', \tag{2}$$

where D_{km} is the mixture-averaged diffusion coefficient, which provides a relation between the mass flux and the mass-fraction gradient, D_k^T is the thermal diffusion coefficient, T is the temperature, and j' is the correction term.

The conservation of energy, under the assumption of negligible viscous effects, is shown in Eq. 3:

$$\rho\frac{\partial T}{\partial t}+\frac{1}{c_p}\sum_{k=1}^{K}\hat{h}_k\dot{\omega_k}+\frac{1}{c_p}\sum_{k=1}^{K}j_k c_{p,k}\frac{\partial T}{\partial x}=\frac{1}{c_p}\frac{\partial}{\partial x}\left[\lambda\frac{\partial T}{\partial x}\right], \tag{3}$$

where λ is the mixture thermal conductivity, c_p and $c_{p,k}$ are the mixture and species specific heat capacities at constant pressure, respectively, and $\hat{h}_k$ is the species molar enthalpy.

3 Problem setup and initial conditions

In the current work, we investigate numerical solutions for 1-D reactive and stagnant diffusion layers under conditions relevant for a pressurized hydrogen jet release scenario. Thus, the initial conditions mimic the conditions for diffusion ignition at the hydrogen jet's head, where one side contains pressurized hydrogen and the other side contains air diluted with nitrogen. The initial conditions are determined according to a 1-D shock-tube solution via the software package Cantera [11]. Note that we do not take into account the jet expansion during the release process itself. This approach provides insights on the fundamental problem dynamics at the early stages before significant jet expansion occurs, see also [12]. For all the cases, a pressure ratio of 400 was assumed between the pressurized hydrogen, in the driver section, and the ambient, in the driven section, with an initial temperature of 293 K for both gases. The domain size is 2 mm and the interface between the two gases is located exactly at the domain's center. Also, we used a uniform grid with 1200 cells and a time step of 1.0×10^{-10} s, which were found to be sufficiently small for capturing the changes in the reaction and diffusion terms. All the simulations were carried out at least until the ignition was achieved. Moreover, we found that by using a mixture averaged diffusion coefficient, we can achieve indistinguishable results in comparison with using the more computationally expensive multi-component diffusion coefficient. For all the simulations, we used the chemical mechanism of Burke et al. [13], which consists of initiation, chain branching and termination reactions.

The initial temperatures and the pressures at the diffusion layer, which were obtained via the shock-tube solution, are shown in Table 1. We investigated three different cases, where, in each case, the ambient air is diluted by a certain amount of nitrogen. The first case involves pure air, whereas the second and the third cases consist of mixtures with mole percentages of 88% $\mathrm{N_2}$ with 12% $\mathrm{O_2}$ and 94% $\mathrm{N_2}$ with 6% $\mathrm{O_2}$, respectively. Pure hydrogen was used as fuel in the three different cases. One can see in Table 1 that the $\mathrm{N_2}$ dilution on the air side has a negligible effect on the initial conditions. For instance, for 21% of $\mathrm{O_2}$, the pressure at the diffusion layer is equal 43.71 atm, and for the most diluted case with 6% of $\mathrm{O_2}$, a value of 43.43 atm is obtained. Hence, the differences between the initial temperatures are also very small. This is not surprising as $\mathrm{N_2}$ and $\mathrm{O_2}$ have very similar molar weights. Next, we present and analyze the resulting temperature and species-mass-fraction evolution for the different cases.

Table 1: Initial temperature and pressure profiles at the diffusion layer for diluted air side obtained from the shock-tube solution for a pressure ratio of 400.

Ambient composition	$\mathrm{H_2}$ **temperature,** K	**Air temperature,** K	**Initial pressure,** atm
21% O_2**, 79%** N_2	150.65	2100	43.71
12% O_2**, 88%** N_2	150.34	2098	43.43
6% O_2**, 94%** N_2	150.14	2097	43.24

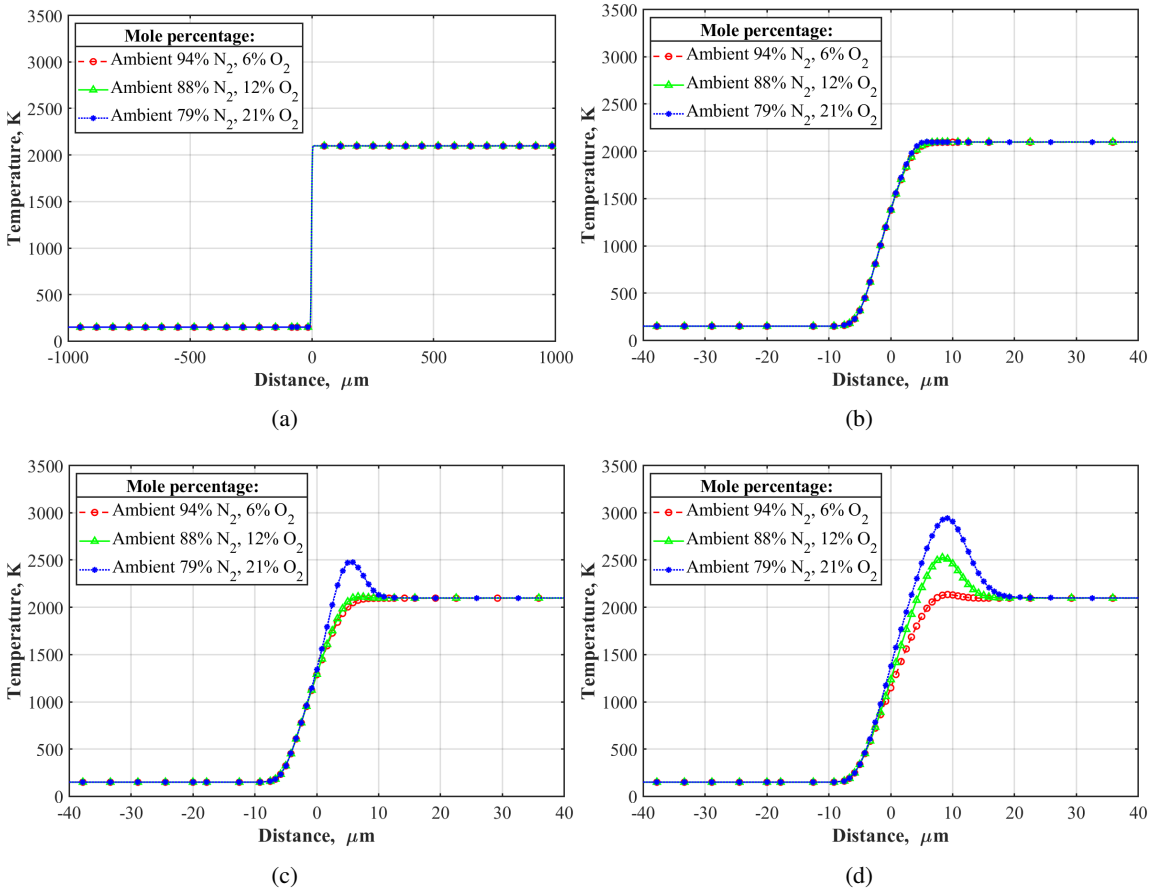

Figure 2: Temperature profiles in the diffusion layer region at (a) t=0 μs, (b) t=0.06 μs, (c) t=0.10 μs, and (d) t =0.20 μs.

4 Results

Figure 2 shows the temperature profiles for all the cases at different time instants. At time t=0 μs, the initial profiles are almost identical, see Fig. 2(a). Note that the nitrogen dilution influence on the initial conditions is negligible due to the almost identical speed of sound for all the cases, which leads to an almost identical shock-wave strength. After 0.06 μs, hydrogen diffuses rapidly within the diffusion layer due to its low molecular weight. The hot air and cold hydrogen mix and heat transfer occurs through conduction. As a result, the hydrogen heats up gradually and starts reacting with the oxygen in the air. As the hydrogen and oxygen react with each other, more heat is released, which further increases the temperature of the mixture and leads to a self-ignition process. The temperature increase or the so-called "hump" shown in Figure 2(b), for the pure-air case, demonstrates the self-ignition process. At 0.10 μs, see Figure 2(c), the diluted case with 12% O_2 undergoes a temperature increase and that leads to self-ignition. Thus, the ignition-delay-time difference between the pure-air case and the 12% O_2 diluted case equals 0.04 μs. Figure 2(d) shows that self-ignition has also occurred for the case with 6% O_2 after 0.20 μs with a time delay difference, in comparison to the pure-air case, of about 0.14 μs. In summary, it is observed that although the last case contained only 6% of O_2, this amount did not delay significantly the self-ignition process in comparison with the undiluted case.

Figure 3 shows OH and H_2O mass fractions at 0.20 μs. According to the chemical reaction mechanism by Burke et al. [13], O_2 and H_2 react and form the radical OH and H_2O in the chain-branching and

termination reactions, respectively. OH is produced first for the pure-air case, followed by the cases of 12% O_2 and 6% O_2, which are shown in Figure 3(a). It is also important to observe the peak positions where the OH is produced. The peak for pure air and the 6% O_2 case are located around the same positions at x=10 μm, whereas the peak of OH for the case with 12% O_2 is located around x=9.17 μm.

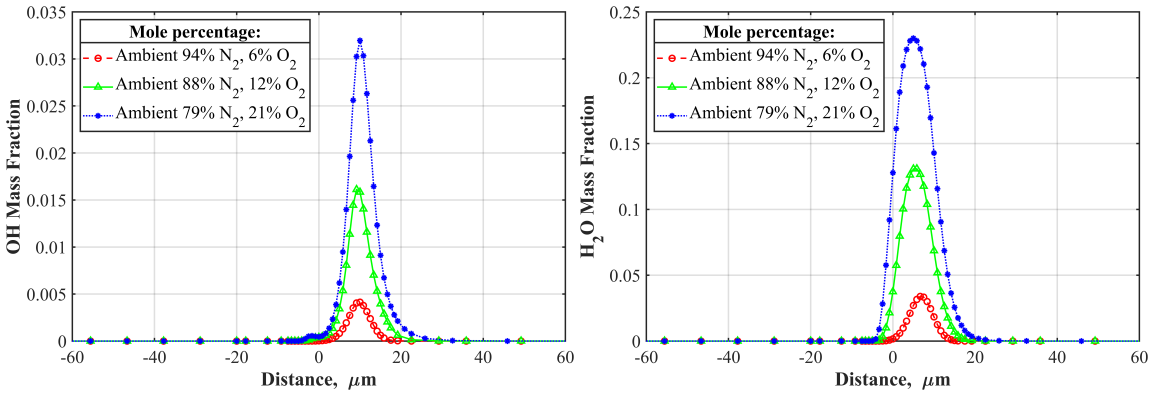

Figure 3: Species mass fraction profiles at t=0.20 μs: (a) OH mass fraction, (b) H_2O mass fraction.

Figure 3(b) shows the production of water as a result of termination reactions, see [13]. Water is produced first in the pure-air case, followed by the 12% O_2 and 6% O_2 cases, respectively. Moreover, H_2O has a higher molar weight than OH; therefore, H_2O has a lower diffusion coefficient than OH [14]. As a result, H_2O diffuses less deep into the hot air region than OH. For example, the peak in mass fraction of H_2O occurs at x=5 μm for both the pure-air case and the 12% O_2 case, and at x=6.67 μm for the 6% O_2 case.

5 Conclusion

The aim of this work is to investigate the self-ignition process of pressurized hydrogen release into atmospheric air diluted with nitrogen. To achieve this goal, we used the open-source code Ember for conducting 1-D unsteady simulations of the mass and heat transfer as well as the chemical reactions at the reactive diffusion layer. The initial conditions mimic a pressurized jet release scenario and are derived by solving a shock-tube problem.

Analysis of the initial temperature profiles shows that nitrogen dilution on the air side has a negligible effect on the shock strength. It is thus demonstrated that the increase in ignition delay time is solely due to the chemical composition of the ambient. Nevertheless, the maximum difference in the ignition delay times, which occurs between the pure air case and the most diluted case with 6% O_2 is about 0.14 μs. Also, analysis of the H_2O and OH mass fractions reveals that the location where the peaks in mass fractions of H_2O and OH occur are not significantly affected by driven-gas dilution.

6 Acknowledgements

The authors would like to acknowledge the NRCN-CEA International Collaboration Research Fund and the Pazy Foundation for funding this research.

References

[1] Rudy W, Teodorczyk A, Wen J. (2017). Self-ignition of hydrogen-nitrogen mixtures during high-pressure release into air. Int. J. Hydrog. Energy. 42: 7340.

[2] Vijayan PK, Kamble MT, Nayak AK, Vaze KK, Sinha RK. (2013). Safety features in nuclear power plants to eliminate the need of emergency planning in public domain. Sadhana. 38: 925.

[3] Wolanski P, Wojcicki S. (1973). Investigation into the mechanism of the diffusion ignition of a combustible gas flowing into an oxidizing atmosphere. Proc. Combust. Inst. 14: 1217.

[4] Maxwell BM, Radulescu MI. (2011). Ignition limits of rapidly expanding diffusion layers: Application to unsteady hydrogen jets. Combust. Flame. 158: 1946.

[5] Golovastov SV, Baklanov DI, Volodin VV, Golub VV, Ivanov KV. (2009). An experimental study of the diffusion-controlled self-ignition of hydrogen in a channel. Russ. J. Phys. Chem. B. 3: 348.

[6] Mogi T, Wada Y, Ogata Y, Hayashi AK. (2009). Self-ignition and flame propagation of high-pressure hydrogen jet during sudden discharge from a pipe. Int. J. Hydrog. Energy. 34: 5810.

[7] Dryer FL, Chaos M, Zhao Z, Stein JN, Alpert JY, Homer CJ. (2007). Spontaneous ignition of pressurized releases of hydrogen and natural gas into air. Combust. Sci. Technol. 179: 663.

[8] Golub VV, Baklanov DI, Golovastov SV, Ivanov MF, Laskin IN, Saveliev AS, Semin NV, Volodin VV. (2008). Mechanisms of high-pressure hydrogen gas self-ignition in tubes. J. Loss Prev. Process. Ind. 21: 185.

[9] Zhou S, Luo Z, Wang T, He M, Li R, Su B. (2022). Research progress on the self-ignition of high-pressure hydrogen discharge: A review. Int. J. Hydrog. Energy. 47: 9460.

[10] Long AE, Speth RL, Green WH. (2018). Ember: An open-source, transient solver for 1D reacting flow using large kinetic models, applied to strained extinction. Combust. Flame. 195: 105.

[11] Goodwin DG, Moffat HK, Speth RL. (2009). Cantera: An object-oriented software toolkit for chemical kinetics, thermodynamics, and transport processes. Caltech, Pasadena.

[12] Bourgin E, Alves MM, Yang C, Fachini FF, Bauwens L. (2017). Effects of Lewis numbers and kinetics on spontaneous ignition of hydrogen jets. Proc. Combust. Inst. 36: 2833.

[13] Burke MP, Chaos M, Ju Y, Dryer FL, Klippenstein SJ. (2012). Comprehensive H2/O2 kinetic model for high-pressure combustion. Int. J. Chem. Kinet. 44: 444.

[14] Turns SR. (2011). An introduction to combustion: Concepts and applications. McGraw Hill.